

A New Cryosurgical Device for Controlled Freezing

I. Setup and Validation Tests

YOED RABIN¹ AND AVRAHAM SHITZER

Department of Mechanical Engineering, Technion-Israel Institute of Technology, Haifa 32000, Israel

A new cryosurgical device utilizing liquid nitrogen, which is a modification of an existing commercial system, was developed. In the new computer-controlled cryodevice the temperature of the cryoprobe is controlled by means of an electrical heating element. The desired temperature-forcing function is calculated to ensure a specified constant cooling rate at the freezing front. The new device facilitates real-time data processing, and, in particular, simulation of the heat transfer processes. A series of tests was performed to study the characteristics of the cryodevice and to validate the underlying assumptions. These tests were performed using organic tissue, i.e., potatoes, as an *in vivo* simulating medium of biological tissue. The differences between experimental data and computed results were found to be within $\pm 0.5^\circ\text{C}$, which falls within the uncertainty range of the experimental temperature measurements. A typical control error of the new device is within $\pm 0.3^\circ\text{C}$, prior to the formation of the freezing front, and $\pm 0.6^\circ\text{C}$ thereafter, which is of the same order of magnitude as the uncertainty range of the temperature measurements. The new device is capable of producing maximal cooling rates of $50^\circ\text{C}/\text{min}$ down to temperatures of -165°C and a maximal heating rate of $300^\circ\text{C}/\text{min}$. The maximal cooling power of the cryoprobe, due to LN_2 boiling, is 80 W; the maximal electrical heating power of the cryoprobe is 160 W. Precooling of the device requires about 30 min, and it can be operated continuously for about 3 h. Initial results of experimental *in vivo* cryosurgery performed on rabbit hindlimbs, including histological observations and thermal analysis, are presented in the second part of this study. © 1996 Academic Press, Inc.

Destruction of undesired biological tissues by freezing, termed cryosurgery, is considered to be an effective medical treatment modality (29, 30). Cryosurgery has several medical and economical advantages, e.g., low bleeding, good esthetic results, minimal use of anesthetics, short period of recovery, and low cost of the procedure (14, 15, 18-20). It has been reported that the cryotreatment often stimulates the immune system and thus activates the natural destruction mechanisms of tumors and prevents their recurrence (1, 10, 32).

A number of factors which determine the success of cryosurgery were suggested in several studies (21, 29). Among them are: the lowest temperature achieved (12), the cooling rate during freezing (8, 13, 31), the thawing rate following the freezing process (17), and the number of repeated freezing/thawing cycles (13, 28).

Several studies have suggested that the cooling rate imposed at the freezing front is one of the most important factors for cell destruction during cryotreatment (9, 20). Indeed, maximal cell destruction may be achieved at very low or, alternatively, at very high cooling rates, due to different modes of destruction mechanisms (16, 20, 21). Similar to the cooling rate effect, it was found experimentally that low thawing rates increase cell destruction as well (2). The factors determining the success of cryotreatment have been examined mainly on cell cultures (16, 17, 20). To the best of our knowledge, experimental studies on the effect of a constant cooling rate prevailing at the freezing front on the survival of living tissue following cryotreatment have not been reported to date.

A new cryosurgical device for *in vivo* experimental cryosurgery has been developed in this study. The objective of the development of the new cryodevice is to facilitate experimental investigations of the above factors on the success of *in vivo* cryotreatments. It is assumed in this study that the cooling rate at the freezing front

Received February 6, 1995; accepted July 25, 1995.

¹ Present address: Division of Surgical Oncology, Allegheny General Hospital, Pittsburgh, PA.

and the repeated freezing/thawing cycles are among the most important factors determining tissue destruction.

The new cryodevice is computer controlled; the controlled variable is the temperature of the cryoprobe. In this study the input function to the control system is calculated to ensure a certain specified low cooling rate at the freezing front. However, the new cryodevice is capable of controlling, within physical limits, faster cooling rates as well. Real-time estimation of freezing front location, by numerical heat transfer simulation, is performed by the computerized cryodevice.

Validation tests of the new cryodevice were performed by comparing experimental data and heat transfer simulation results of cryoprocures. The characteristics of the new cryodevice were investigated by performing a large number of experiments. Both series of test were performed on potatoes, simulating cryosurgical processes under various conditions. The new cryodevice was found to be suitable for *in vivo* experimental cryosurgery, as is presented in the second part of this study (23).

DESCRIPTION OF THE NEW CRYODEVICE

The new cryodevice is an upgrade of an ear-

lier version, which was used for experiments on inanimate materials, simulating biological tissues (4). The upgrading of the new device involved mainly the following: 1) adjustment of the cryodevice to *in vivo* cryosurgery, including temperature measurements inside the cryotreated tissue; 2) improvement of the closed-loop control system by increasing the cooling power and decreasing the controlled variable error; 3) improvement of the method for calculating the temperature forcing function by developing new mathematical solutions, which take into account repeated freezing/thawing cycles, and the thermal effects of blood perfusion and metabolic heat generation; and 4) improved estimation of the interface location, or the penetration depth of the cryotreatment, by real-time data processing and numerical heat transfer simulation.

The new cryodevice is presented schematically in Fig. 1, basically following the system originally developed by Budman *et al.* (4, 5). Four subsystems may be identified: 1) the cryo-fluid unit, generating the heat sink of the cryoprobes; 2) the power amplifier and the electrical heater, generating the heat source of the cryoprobe; 3) the temperature measurement unit; and 4) the microcomputer, which embodies a

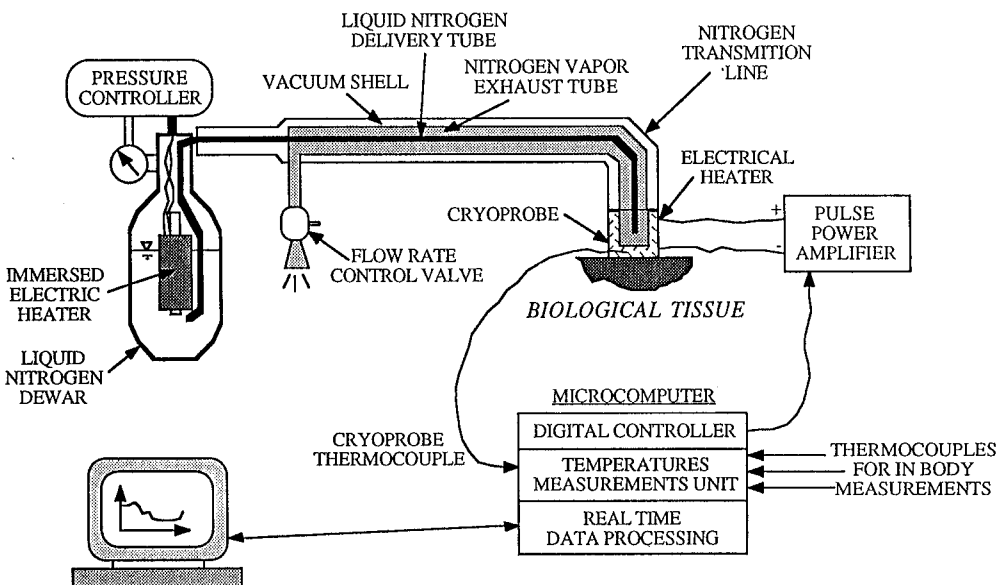


FIG. 1. Schematic presentation of the cryosurgical device.

digital controller and a real-time data processor. These subsystems are described subsequently in more detail.

The cryofluid subsystem was modified from a commercial cryosurgical cooling unit (Ricor Ltd., Israel, model C3-13A). The cryofluid, liquid nitrogen (LN_2), is stored in a vacuum-insulated dewar which is pressurized by an immersed heater. The LN_2 is forced into the cryoprobe through a vacuum-insulated delivery tube at a rate dependent on the pressure in the dewar. Inside the cryoprobe, which is in contact with the cryotreated tissue, the LN_2 boils and acts as a heat sink. The nitrogen vapors produced at the cryoprobe return through an annular space between the supply tube and the vacuum insulation. During the entire process, a constant flow rate of LN_2 is maintained by means of a valve which controls the release of the N_2 vapor. Thus, an independent constant power heat sink is generated in the cryoprobe.

The actual cooling power of the cryoprobe is very difficult to measure experimentally due to the unstable LN_2 boiling regime inside the cryoprobe and convection heat transfer from the surroundings to the cryoprobe. However, the upper bound of the cooling power may be estimated by multiplying the mass flow rate of LN_2 and its latent heat of boiling, which yields in this case a cooling power of 80 W. The actual cooling power decreases with the decreasing of cryoprobe temperature, as the convection heat transfer from the surroundings increases and as the temperature difference between the cryoprobe and the boiling temperature of LN_2 decreases. In general, it can be assumed that the cooling power decreases exponentially with temperature, where its value at a cryoprobe temperature

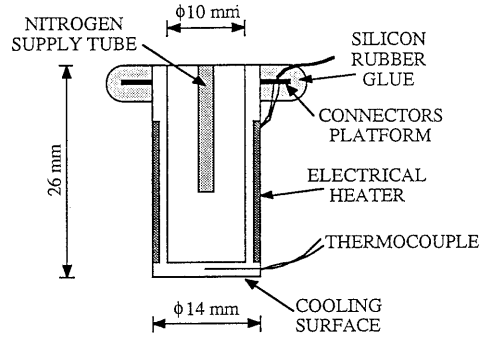


FIG. 2. Cross-section of the brass cryoprobe and details of its thermocouple arrangement. Dimensions are in mm. Modified from Budman *et al.* (4).

of -165°C is about one third of its value when the cryoprobe is at room temperature (22).

As was first suggested by Filippi (11) and adopted by Budman *et al.* (4), the temperature of the cryoprobe is controlled using an electrical heater wound around its outer surface (Philips Thermcoax, Class A, Type NcAc 10, 1-mm O.D.) as shown schematically in Fig. 2. The cryoprobe was designed and manufactured in our own laboratory. By controlling the power supplied to the cryoprobe, while the cryofluid produces a constant heat sink, the temperature of the cryoprobe may be controlled at the desired values. Thus, the heat supplied to the electrical heater is actually the controlled variable of the closed-loop controlling system (Fig. 3).

The power supply of the electrical heater wound around the cryoprobe is a simple pulse power amplifier manufactured in our own laboratory. It is designed for periodic outputs of maximal and zero power, which is suitable for amplifying the digital output of the digital con-

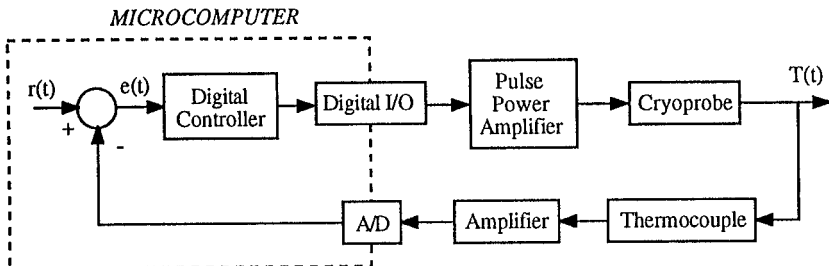


FIG. 3. Schematic presentation of the control loop in the new cryodevice.

troller (materialized by a microcomputer). Amplifying the controller output without any type of D/A converter eliminates potential controlling errors at this stage and thus improves the performance of the control system with respect to the one used in the earlier device (4). The effective power supplied to the electrical heater is given by

$$q_{\text{eff}} = \frac{\tau_{\text{max}}}{\tau_{\text{cyc}}} \cdot q_{\text{max}} \quad [1]$$

where the maximal power period, τ_{max} , is constant, and the cycling period, τ_{cyc} , is determined by the digital controller. Additional nomenclature is shown in Table 1. The maximal installed power supply is 160 W, which is twice the maximal cooling power of the cryofluid heat sink. A factor of 2 is required for fast cryoprobe heating at the end of the treatment, or in case of an emergency, for quick detachment of the cryoprobe from the tissue surface. Due to safety requirements the maximal voltage of the power amplifier is set at 40 VAC.

The temperature measurement unit consists of 10 channels of copper–constantan thermocouples as follows: 1) a cryoprobe temperature channel, which is used as the main feedback of the closed-loop control system (Fig. 3); 2) an independent channel of the cryoprobe temperature (floating channel) connected to an alarm microsystem, due to safety requirements; 3) a surrounding temperature channel, which is the reference temperature (cold junction compensation); and 4) seven channels for temperature

measurements inside the tissue. All thermocouples were manufactured from Waltow Gordon's, USA, copper–constantan wires, gauges 24 (0.51 mm) and 36 (0.13 mm), catalog nos. T24/1/505 and T36/2/506, respectively.

All temperature channels, except for the cryoprobe temperature alarm, are amplified by a gain factor of 500, by insulated amplifiers (Megatron Ltd., Israel) with at least 99.9% linearity, designed especially for this purpose. The amplified analog signals are converted into digital signals using a 12-bit A/D convertor and a 9-channel multiplexer in one unit (Eagle Technology, Cape Town, S. Africa, model PC-73). The digital signals are converted into numerical values of temperatures by the control program using an eight-power polynomial, which provides a very accurate and a very fast conversion. It is noted that under cryogenic conditions, amplifying the copper–constantan thermocouple signals by a gain factor of 500 leads to a 75% utilization ratio of the maximal microcomputer input, ± 4 V. Using this large amplifying gain factor reduces the error caused by the A/D conversion. The uncertainty of the temperature measurements, as estimated by the square root of the sum of squares of the individual uncertainties, is $\pm 0.53^\circ\text{C}$. This value is obtained by the following uncertainty values: amplifier $\pm 0.1^\circ\text{C}$, A/D convertor $\pm 0.1^\circ\text{C}$, an eight-power polynomial conversion $\pm 0.1^\circ\text{C}$, and the thermocouple error $\pm 0.5^\circ\text{C}$.

The accuracy of the cryoprobe temperature measurement is of great importance since it is used as the feedback variable for closing the control loop. The cryoprobe is actually the junction of the cryofluid unit, the power unit, and the temperature measurement unit. The cryoprobe temperature is measured near the surface which is in contact with the biological tissue. The cryoprobe used for the experimental system, shown schematically in Fig. 2, is a typical commercial probe for surface cryotreatment applications. Additional technical information concerning the cryoprobe is given by Budman *et al.* (4).

The floating cryoprobe alarm channel is designed to activate a beeper whenever a prespeci-

TABLE 1
Nomenclature

e	Controlling loop error ($^\circ\text{C}$)
KI	Integration gain of the controller (W/s- $^\circ\text{C}$)
	Proportional gain factor of the controller
KP	(W/ $^\circ\text{C}$)
q	Electrical heater power (W)
t	Time (s)
τ	Period (s)
Subscripts	
cyc	Cycle of the controller
eff	Effective
i	Time counter
max	Period in which maximal power is obtained

fied temperature is exceeded. This channel uses a dedicated electrical source (batteries), a simple linear amplifier, a read-relay, a beeper, and a copper-constantan thermocouple. The alarm temperature can be set by a rheostat in the range of 40–100°C.

The core unit of the new cryosurgical device is an IBM-PC-compatible microcomputer, with a 80486/33MHz microprocessor. The microcomputer is used for five tasks: 1) temperature monitoring; 2) real-time data processing; 3) proportional-integral (PI) digital controlling; 4) data logging; and 5) graphical and numerical display of data. A computer software, Cryoprobe Control Program (CCP), was written specifically for performing these tasks simultaneously, using Turbo Pascal 5 and Turbo Assembler 2 compilers. The CCP as a real-time data processor is used for the calculation of the desired temperature-forcing function of the cryoprobe and for the estimation of freezing front location.

As indicated above, it is assumed that the control of the cooling rate at the freezing front is one of the most important factors determining the success of cryotreatment. The desired cryoprobe temperature-forcing function, $r(t)$ in Fig. 3, that would lead to a constant cooling rate at the freezing front, is obtained as the solution of an inverse Stefan problem in biological tissue (25). It can be shown mathematically that there does not exist a general solution to the multidimensional inverse Stefan problem. However, it can also be shown that a solution to the one-dimensional inverse Stefan problem is the upper bound for the freezing front location and for the cooling rate at the freezing front, all with respect to a multidimensional problem having the same temperature-forcing function at the interface with the cryoprobe. Since a low cooling rate at the freezing front is desired as it causes deeper penetration of the freezing front, and since it is assumed that tissue destruction increases with the decreasing of the cooling rate (17), the one-dimensional solution is applied here. The temperature-forcing function can be calculated by an exact solution for the first freezing/thawing cycle (26), for a problem hav-

ing a uniform initial condition. Alternatively, it can be calculated by a combined solution (25) for repeated freezing/thawing cycles and for a nonuniform initial condition. It is noted that the exact solution can be calculated *a priori* while the combined solution must be calculated in real time, simultaneously with the application of the cryoprocure.

The location of the freezing front in the tissue can be calculated using a multidimensional finite difference numerical scheme (24, 27). The numerical scheme calculates the temperature field in the tissue, and the freezing front location has to be interpolated from it. The temperature field in the tissue, resulting from a superficial cryotreatment, can be assumed two-dimensional and axi-symmetric. However, the use of a 80486/33MHz microprocessor, for real-time heat transfer simulations as well as for controlling the cryodevice, allows only one-dimensional numerical solutions. Upgrading the system to a faster microprocessor will enable simulations of two-dimensional problems.

The CCP integrates the above mathematical solutions with the digital controller. First, the CCP calculates the desired forcing function by the exact or by the combined solutions mentioned above. Second, the CCP measures the cryoprobe temperature. Last, the CCP calculates the digital controller output by the difference between the two values. As was suggested and discussed by Budman *et al.* (4, 5), a PI controller is used.

$$q_i = q_{i-1} + KP(e_i - e_{i-1}) + KI \frac{\tau}{2}(e_i + e_{i-1}) \quad [2]$$

The proportional gain factor KP and the integral gain factor KI were selected based on the results of a dynamic simulation of the cryoprocess. Fine tuning of these parameters was performed experimentally. It was found that the new gain parameters of the upgraded system do not differ much from the earlier ones. However, it was found experimentally that slightly different gain values are better suited for different cryoprobe temperatures. These differences result from changes in the LN₂ boiling regime occurring

during the lowering of the cryoprobe temperature. Thus, the CCP enables interactive modifications of controller gain parameters during the cryoprocure.

The digital output of the controller (Eagle Technology, model PC-14B extension board of the microcomputer) is amplified by a pulse power amplifier. Two independent timers/counters, 16-bit counting each, produce independent periodic digital outputs. While the cycling period of the digital output remains unchanged during the entire operation (first counter), the CCP may still change the maximal power period (second counter) according to the control law, Eq.[2]. Thus, the microprocessor is available, for most of the time, for the other CCP assignments. Using on board a 2-MHz reference oscillator for the timers/counters, 25-ms cycling period, and 16-bit conversion of numerical values to digital outputs, the conversion error added to the control loop at this stage can be neglected (estimated at less than 0.002%). An additional timer/counter and a digital I/O channel are used for the synchronization between the controlling loop and the real-time data processing, including the calculations of the forcing function, the heat transfer simulation, and the data processing and storage.

In addition to its functioning during the cooling process, the CCP handles pre- and postcryosurgery procedures. During the pre-process, the cryoprobe temperature is stabilized at an initial value, equal to the unperturbed tissue temperature. At this stage the cryofluid is already flowing to cool the system while the patient is being

prepared for the cryotreatment. During the post-process, the cryoprobe temperature is stabilized again at the same level. At this stage the cryoprobe is detached from the tissue. Fig. 4 presents the general flow chart of the CCP.

VALIDATION TESTS AND SYSTEM CHARACTERISTICS

Validation tests of the new cryodevice have been performed by applying the cryotreatment to organic tissues, i.e., potatoes. Potatoes were chosen as the simulation medium since their thermophysical properties are close to those of a biological tissue *in vivo* (3, 6, 7), Table 2. It is noted that the organic tissue of a potato can be treated as a homogeneous and isotropic medium, with regard to heat transfer calculations. In contrast, the living biological tissue can only be approximated as such in cases of peripheral tissues and particularly in regions close to the external surface. The objectives of the validation tests were: 1) to compare the computer simulation results and experimental data of the temperature field; 2) to fine tune the controller gains under various working conditions, e.g., cooling rates and cryoprobe temperatures; and 3) to examine system characteristics.

The comparison between the computer simulation and the experimental data was performed using a one-dimensional freezing problem. A schematic description of the experimental setup for a one-dimensional heat transfer is shown in Fig. 5. Typical results from one of 16 freezing experiments are presented. This experiment was performed under the following conditions: con-

TABLE 2
Typical Thermophysical Properties of a Healthy Muscle Tissue and a Potato (6, 7)

Thermophysical property	Healthy muscle tissue	Potato
Upper bound of freezing	-1°C	-1°C
Peak of phase transition temperature	-3°C	-3°C
Lower bound of freezing	-8°C	-8°C
Thermal conductivity in unfrozen region	0.48 W/m-°C	0.45 W/m-°C
Thermal conductivity in frozen region	1.68 W/m-°C	2.00 W/m-°C
Volumetric specific heat in unfrozen region	3.16 MJ/m ³ -°C	3.52 MJ/m ³ -°C
Volumetric specific heat in frozen region	1.80 MJ/m ³ -°C	1.84 MJ/m ³ -°C
Latent heat of solidification	233.4 MJ/m ³	268 MJ/m ³
Product of blood perfusion and its specific heat	2.5 kW/m ³ -°C	

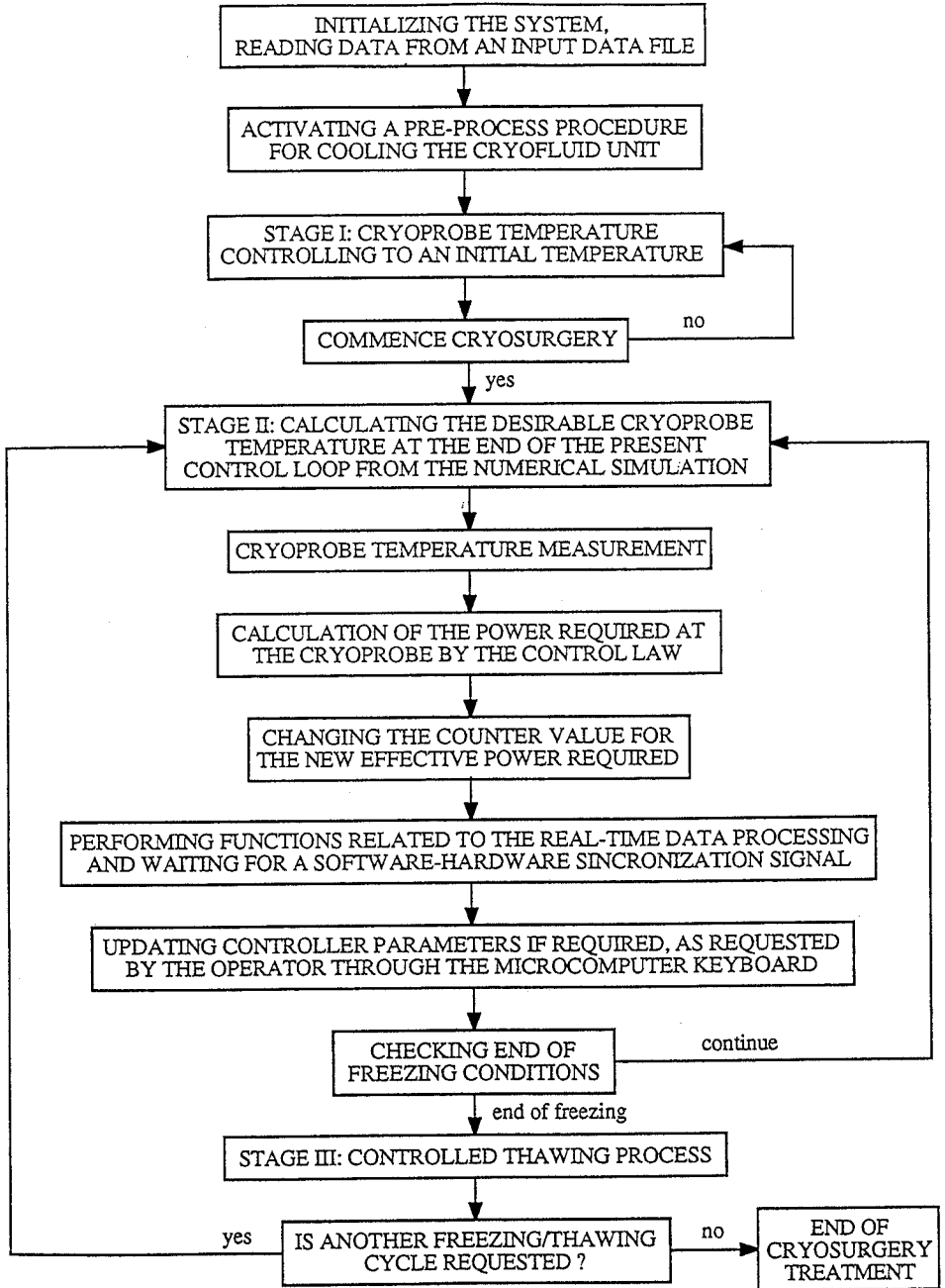


FIG. 4. Flowchart of the CCP.

stant cooling rate at the freezing front of $12.5^{\circ}\text{C}/\text{min}$, minimal cryoprobe temperature of -100°C , and a uniform initial condition of 17.4°C . Thermophysical properties taken for

the computer simulation are summarized in Table 2. The computer simulation results were calculated using the following assumptions. 1) The thermal conductivity is linearly dependent

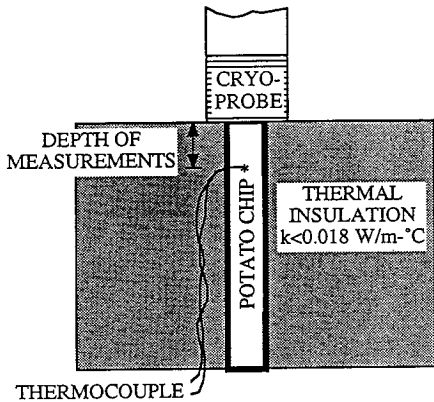


FIG. 5. Schematic presentation of the experimental setup for one-dimensional freezing in a potato.

on the temperature in the phase transition range. 2) The volumetric specific heat is dependent on the temperature in the phase transition range, having two different slopes above and below the peak temperature of phase change (26). 3) Space intervals are 0.125 mm in the numerical solution (27). 4) The forcing function for the computer simulation was taken as the measured cryoprobe temperature during the experiment.

Good agreement between numerical results and experimental data, at a depth of 7.7 mm below the surface of the cryoprobe, can be seen in Fig. 6. The temperature of the cryoprobe is almost linear for a cooling rate of 12.5°C/min at

the freezing front. Fig. 7 presents the differences between the measured data and the numerical results at the same depth. It can be seen that the average difference in the unfrozen region is about -0.3°C, while the average difference in the frozen region is about +0.25°C. The differences between the simulation results and the experimental data are within the range of the uncertainty of the data measurements. Relatively large differences are observed within the phase transition temperature range, most likely due to the uncertainty in the values of the thermophysical properties and the inherent instability of the thermodynamic process in this range. While examining the results presented in Figs. 6 and 7, the following factors have to be taken into account. 1) There is uncertainty of about ±0.53°C in temperature measurements. This uncertainty is related to the measurement point at 7.7 mm depth as well as to the temperature of the cryoprobe. However, the measured cryoprobe temperature was taken as an exact value for the computer simulation. 2) There is an uncertainty of about 10% in the values of the thermophysical properties listed in Table 2. 3) There is additional uncertainty in the location of the temperature sensor. A reasonable error of 0.1 mm in sensor placement will contribute an uncertainty of about ±0.7°C in the temperature measurement.

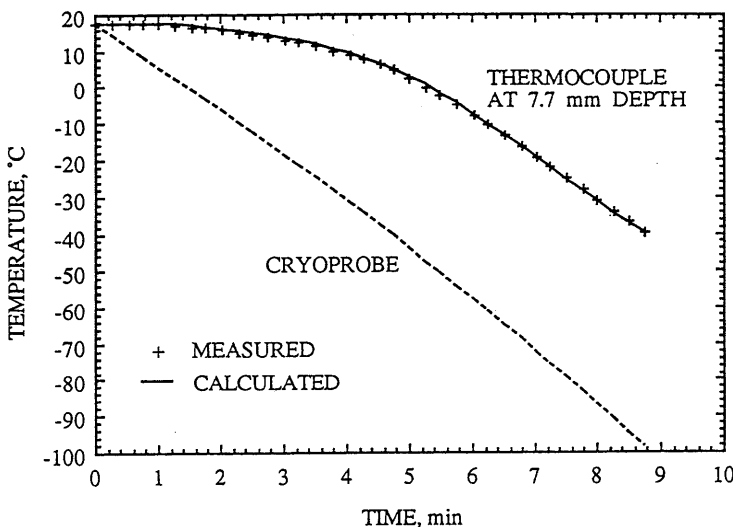


FIG. 6. Comparison of numerical results and experimental data in a potato at 7.7-mm depth.

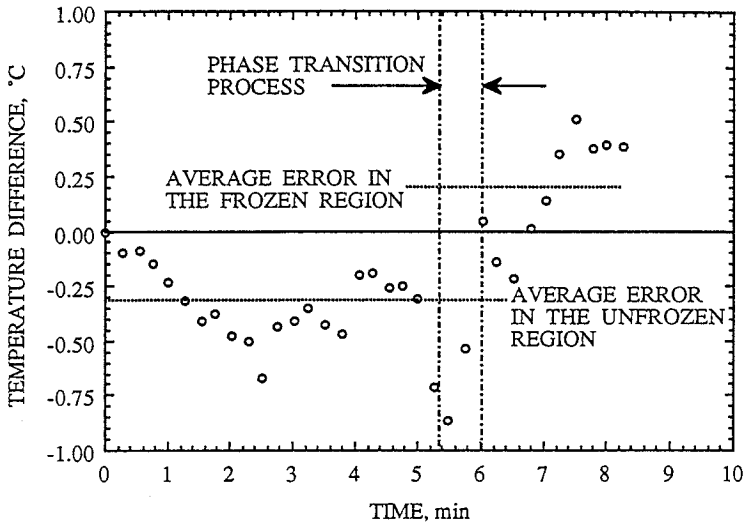


FIG. 7. Differences between measured data in a potato (O) and the computed results at 7.7-mm depth.

From the comparison of the numerical results and the experimental data, taking into account the above factors of measurement uncertainty, it can be deduced that the computer simulation is a good and reliable engineering tool for estimating the temperature field and thus for predicting the location of the phase change interface.

System characteristics were examined using 24 simulations of cryoprocesses on potatoes under various operating conditions. The following system characteristics have been obtained from these experiments. 1) The lowest cryoprobe temperature that can be achieved is -193°C . 2) The highest constant cooling rate of the cryoprobe in contact with the tissue is about $50^{\circ}\text{C}/\text{min}$. 3) The highest cooling rate for the cryoprobe suspended in free air is about $400^{\circ}\text{C}/\text{min}$. 4) The highest heating rate for the cryoprobe in contact with the tissue, at maximal cryofluid flow rate, and an initial cryoprobe temperature of -165°C , is about $300^{\circ}\text{C}/\text{min}$. 5) Free thawing by natural convection with a warm environment leads to thawing rates of a few degrees Celsius/min, which enhances the destruction of the tissue (17). 6) The cryofluid unit needs to be cooled for about 30 min prior to the cryotreatment. The precooling is required to reduce the extent of nitrogen evaporation through the pipes once the cryoprobe is brought into contact with the biological tissue, such that a higher cooling

rate and a constant heat sink can be obtained. 8) The system can be operated continuously for about 3 h, while the duration of a typical cryotreatment procedure is from 10 to 25 min. 9) The optimal controller gain parameters are: $KP = 6\text{W}/^{\circ}\text{C}$ and $KI = 3\text{W}/\text{s}\cdot^{\circ}\text{C}$. 9) The control error, $e(t)$, is within the range of $\pm 0.3^{\circ}\text{C}$ prior the formation of the freezing front and $\pm 0.6^{\circ}\text{C}$ thereafter. This controlling error is related to the differences that were measured by the computer and does not take into account the uncertainty of the measurements. It can be seen that the controlling error is of the same order as the uncertainty of the temperature measurements. 10) An overshoot of about 1.5°C followed by an undershoot of about 1.0°C appears when the cryoprobe temperature is within the range -4°C to -5°C . This is due to the phenomenon of supercooling prior to crystallization followed by a sudden increase in temperature at the beginning of the freezing front formation. As is presented in the second part of this paper (23), a similar phenomenon, in the same temperature range, was observed in the *in vivo* experiments with an overshoot of about 2.3°C to 2.6°C , followed by an undershoot of 1.1°C to 1.4°C .

SUMMARY AND CONCLUSIONS

A new cryodevice for experimental cryosur-

gery has been developed for examining the factors determining the success of cryotreatment. Special emphasis was placed on examining the effect of the cooling rate at the freezing front. The new cryodevice is essentially an upgrading of an earlier version (4), used for heat transfer experiments in inanimate materials.

The computer-controlled temperature-forcing function of the cryoprobe is obtained as the solution of a one-dimensional inverse Stefan problem. This solution ensures that the cooling rate at the freezing front is equal to or less than a preselected value. A cooling rate of $12.5^{\circ}\text{C}/\text{min}$ at the freezing front is assumed for demonstration purposes. The CCP, developed in this study, performs real-time data processing for the calculation of the cryoprobe forcing function and for the simulation of the temperature field in the tissue. A PI digital controller is materialized by the CCP.

Validation tests and experimental system characteristics are presented. It was found that the average error between experimental data and simulation results is about -0.3°C in the temperature range above freezing; beyond freezing the error is about $+0.25^{\circ}\text{C}$. The agreement between the computer simulation results and the experimental data is within the temperature measurement uncertainty of the experimental system, i.e., $\pm 0.53^{\circ}\text{C}$.

It was also found that the highest constant cryoprobe cooling rate achievable is about $50^{\circ}\text{C}/\text{min}$, down to a temperature of about -165°C . The cryoprobe controlling error was found to be within the range of $\pm 0.3^{\circ}\text{C}$ prior to the formation of the freezing front and $\pm 0.6^{\circ}\text{C}$ thereafter. An overshoot of about 1.5°C followed by an undershoot of about 1.0°C appears when the cryoprobe temperature is within the range of -4°C to -5°C , due to the phenomenon of supercooling. Higher overshoot values were observed in the *in vivo* experiments.

The application of the new cryodevice to *in vivo* experimental cryosurgery is reported in the second part of this study (23).

ACKNOWLEDGMENTS

This study was supported in part by the James H. Belfer

Chair in Mechanical Engineering and by the fund for the promotion of research at the Technion.

REFERENCES

1. Ablin, J. R., and Fontana, G. Cryoimmunotherapy: Continuing studies toward determining a rational approach for assessing the candidacy of the prostatic cancer patient for cryoimmunotherapy and postoperative responsiveness. *Eur. Surg. Res.* **11**, 223–233, (1979).
2. Akhtar, T., Pegg, D. E., and Foreman, J. The effect of cooling and warming rates on the survival of cryopreserved L-cells. *Cryobiology* **16**, 424–429, (1979).
3. Altman, P. L., and Dittmer, D. S. "Respiration and Circulation." Federation of American Societies for Experimental Biology, Bethesda, MD, 1971.
4. Budman, H. M., Dayan, J., and Shitzer, A. Controlled freezing of non-ideal solutions with application to cryosurgical processes. *ASME J. Biomech. Eng.* **113**, 430–437, (1991).
5. Budman, H., Dayan, J., and Shitzer, A. Control of the cryosurgical process in non-ideal materials. *IEEE Trans. BME* **38** **11**, 1141–1153, (1991).
6. Bonacina, C., Comini, G., Fasano, A., and Primicerio, M. On the estimation of thermophysical properties in nonlinear heat conduction problems. *Int. J. Heat Mass Transfer* **17**, 861–867, (1974).
7. Chato, J. C. Measurement of thermal properties of biological materials. In "Heat Transfer in Medicine and Biology" (A. Shitzer and R. C. Eberhart, Eds.), pp. 167–189. Plenum, New York, 1985.
8. Fahy, G. M. Analysis of "solution effect" injury: Cooling rate dependence of the functional and morphological sequelae of freezing in rabbit renal cortex protected with dimethyl sulfoxide. *Cryobiology* **18**, 550–570, (1981).
9. Farrant, J. Cryobiology: The basis for cryosurgery. In: "Cryogenics in Surgery" (H. von Leden and W. G. Cahan, Eds.), Lewis, London, pp. 15–42 1971.
10. Farrant, J., and Walter, C. A. Cryobiological basis for cryosurgery. *J. Dermatol. Surg. Oncol.* **3**, 403–407, (1977).
11. Filippi, M. Esperienze di termoregolazione in sonde criochirurgiche con capillare. Proceedings, IV World Congress, San Remo, August 20, 1980.
12. Gage, A. A. Critical temperature for skin necrosis in experimental cryosurgery. *Cryobiology* **19**, 273–281, (1982).
13. Gage, A. A., Guest, K., Montes, M., Caruna, J. A., and Whalen, D. A., Jr. Effect of varying freezing and thawing rates in experimental cryosurgery. *Cryobiology* **22**, 175–182, (1985).
14. Macleod, J. H. In defense of cryotherapy for hemorrhoids: A modified method. *Dis. Colon Rectum* **25**, 332–335, (1982).
15. Marcove, R. C. A 17-year review of cryosurgery in the

- treatment of bone tumors. *Clin. Orthop. Relat. Res.* **16**, 231–234, (1982).
16. McGrath, J. J. Low temperature injury processes. In “Advances in Bioheat and Mass Transfer” (R. B. Roemer, Ed.), American Society of Mechanical Engineers, New Orleans, HTD-268, pp. 125–132, 1993.
 17. Miller, R. H., and Mazur, P. Survival of frozen–thawed human red cells as a function of cooling and warming velocities. *Cryobiology* **13**, 404–414, (1976).
 18. Oh, C. One thousand cryohemorrhoidectomies: An overview. *Dis. Colon Rectum* **24**, 613–617, (1981).
 19. Onik, G. New advances in cryosurgery. Paper presented at the International Mechanical Engineering Congress and Exposition, American Society of Mechanical Engineers, Chicago, IL, November 6–11, 1994.
 20. Orpwood, R. D. Biophysical and engineering aspects of cryosurgery. *Phys. Med. Biol.* **26**, 555–575, (1981).
 21. Pasquale, D. Cryosurgery: The present and the future. American Society of Mechanical Engineers, Washington DC, 81-WA/HT-54, 1981.
 22. Rabin, Y. Destruction of biological tissues by controlled freezing. D.Sc. Thesis, Technion–Israel Institute of Technology, Haifa, Israel (1994) (in Hebrew).
 23. Rabin, Y., Coleman, R., Mordohovich, D., Ber, A., and Shitzer, A. A new cryosurgical device for controlled freezing. Part II. *In vivo* experiments on rabbit hindlimbs. *Cryobiology* **33**, 93–105, (1996).
 24. Rabin, Y., and Korin, E. An efficient numerical solution for the multidimensional solidification (or melting) problem using a microcomputer. *Int. J. Heat and Mass Transfer* **36**, 673–683, (1993).
 25. Rabin, Y., and Shitzer, A. Combined solution of the inverse Stefan problem in non-ideal biological tissues. In “Fundamentals of Biomedical Heat Transfer” (M. A. Ebadian and P. H. Oosthuizen, Eds.), American Society of Mechanical Engineers, Chicago, HTD-295, pp. 1–3 1994.
 26. Rabin, Y., and Shitzer, A. Exact solution to the one-dimensional inverse Stefan problem in non-ideal biological tissues. *ASME Heat Transfer* **117**, 425–431, (1995).
 27. Rabin, Y., and Shitzer, A. An efficient numerical solution for the multidimensional freezing (or thawing) in non-ideal biological tissue. Submitted for publication (1995).
 28. Rand, R. W., Rand, R. P., Eggerding, F. A., Field, M., Denbesten, L., King, W., and Camici, S. Cryolymphectomy for breast cancer: An experimental study. *Cryobiology* **22**, 307–318, (1985).
 29. Rubinsky, B. Recent advances in cryopreservation of biological organ and in cryosurgery. Proceedings of the 8th International Heat Transfer Conference, pp. 307–316, 1986.
 30. Shepherd, J., and Dawber, R.P. R. The historical and scientific basis of cryosurgery. *Clin. Exp. Dermatol.* **7**, 321–328, (1982).
 31. Smith, J. J., and Fraser, J. An estimation of tissue damage and thermal history in the cryolesion. *Cryobiology* **11**, 139–147, (1974).
 32. Yantorno, C., Riera, C. M., and Faillaci, M. G. Immunopathological studies on cryoimmunisation of the rabbit male accessory glands. *J. Pathol.* **114**, 39–46, (1979).